Neutral Au$_n$ (n=3-10) Cluster Catalyzes Acetylene Hydrochlorination: A Density Functional Theory Study

Yang Wang, Mingyuan Zhu, Lihua Kang*, Bin Dai*

College of Chemistry and Chemical Engineering/ Key Laboratory for Green Processing of Chemical Engineering of Xinjiang Bingtuan. Shihezi University, Shihezi, Xinjiang, 832000, PR China

1 Structural and electronic properties of gold clusters

Reports on the geometrical configurations of different Au clusters are extensive[1-6]. Regarding the optimal configuration of the Au$_{3-10}$ cluster, numerous researchers concur on a planar structure, and the geometries in our paper are the same with their conclusions (Fig. S1). The most stable configuration of the Au$_9$ cluster in literature[1,3,4] was considered to be isosceles trapezoid. However, D. Xia et al.[6] argued that the arrow-shaped configuration is the most stable. We performed optimization calculations on the two configurations, and we also found that the most stable
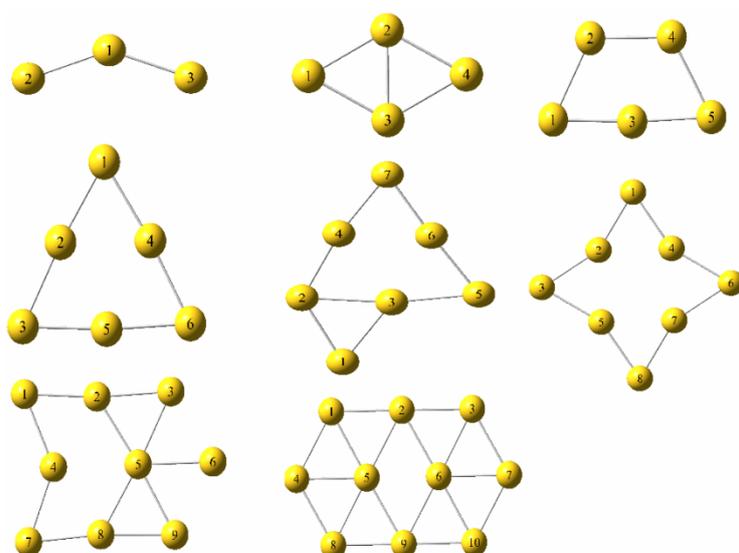

Fig. S1. Optimized geometries of the most stable neutral Au$_n$ clusters (n=3-10).
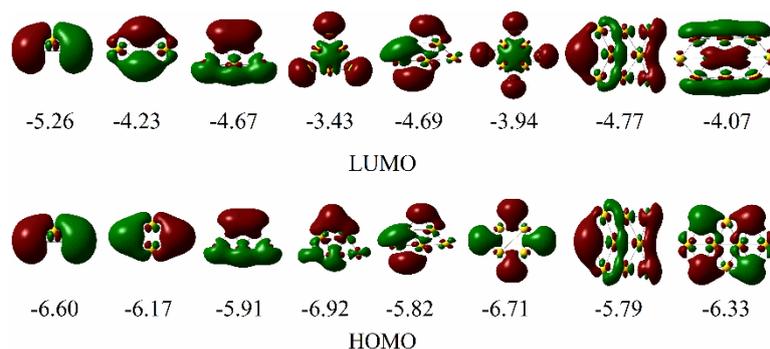
| -5.26 | -4.23 | -4.67 | -3.43 | -4.69 | -3.94 | -4.77 | -4.07 |

LUMO

| -6.60 | -6.17 | -5.91 | -6.92 | -5.82 | -6.71 | -5.79 | -6.33 |

HOMO

Fig. S2. Frontier molecular orbitals and corresponding orbital energies of the neutral Au$_n$ clusters (n=3-10) calculated at the B3LYP/LANL2DZ level of theory. (energies in eV, isovalue = 0.02)

configuration of the Au$_9$ cluster is the arrow-shaped configuration. The FMO and corresponding orbital energies of the neutral Au$_n$ clusters (n=3–10) were calculated and shown in Fig. S2. We then calculated the energy gaps of HOMO–LUMO (Au$_n$→C$_2$H$_2$/HCl) and HOMO–LUMO (C$_2$H$_2$/HCl→Au$_n$) in Table S1. The energy gaps of HOMO–LUMO (HCl→Au$_n$) are smaller than those of HOMO–LUMO (Au$_n$→HCl), and those of C$_2$H$_2$ are the same with those of HCl. These results indicate that both HCl and C$_2$H$_2$ are electron donors and the Au$_n$ clusters are electron acceptors: the electrons transfer from the HOMO of HCl and C$_2$H$_2$ to the LUMO of Au$_n$ clusters. Therefore, we can preliminarily predict the distribution of reaction sites from the LUMO of the Au$_n$ clusters in Fig. S2. We can derive the following information: 1) two different types of active sites exist, namely, top sites (Au$_3$, Au$_4$, Au$_6$, Au$_7$, Au$_8$, Au$_9$) and bridge sites (Au$_5$, Au$_7$, Au$_9$, Au$_{10}$). 2) a high similarity in distribution of reaction sites exists between Au$_6$ and Au$_8$, Au$_5$ and Au$_{10}$. We believe that apart from the size of gold clusters, different types of active sites can affect the catalytic activity

performance. In Fig. S3, we compared the energy gaps of HOMO–LUMO (HCl→Au_n) and HOMO–LUMO (C_2H_2→Au_n) and yielded the following two main results: 1) for

Table S1. The orbital energies on LUMO and HOMO of C_2H_2, HCl and Au_n cluster, and their different energy gaps between C_2H_2, HCl and Au_n cluster. (energies in eV, isovalue = 0.02)

	LUMO	HOMO	HOMO-LUMO (HCl→Au_n)	HOMO-LUMO (Au_n→HCl)	HOMO-LUMO (C_2H_2→Au_n)	HOMO-LUMO (Au_n→C_2H_2)
HCl	-0.81	-9.19				
C_2H_2	0.11	-8.08				
Au_3	-5.26	-6.60	3.93	5.78	2.82	6.70
Au_4	-4.23	-6.17	4.96	5.35	3.85	6.27
Au_5	-4.67	-5.91	4.53	5.10	3.42	6.02
Au_6	-3.43	-6.92	5.76	6.10	4.65	7.02
Au_7	-4.69	-5.82	4.50	5.00	3.39	5.92
Au_8	-3.94	-6.71	5.25	5.90	4.14	6.82
Au_9	-4.77	-5.79	4.42	4.98	3.31	5.90
Au_{10}	-4.07	-6.33	5.13	5.52	4.02	6.44

both HCl and C_2H_2, the energy gaps of even-numbered Au_n clusters are larger than those on adjacent odd-numbered ones, and 2) overall, the energy gaps of HOMO–LUMO (HCl→Au_n) are larger than those of HOMO–LUMO (C_2H_2→Au_n) for even-numbered ones. The energy gaps denote the ability of the electrons to transfer

between HCl/C_2H_2 and Au_n clusters. Therefore, we can predict that acetylene adsorption is better on gold clusters than on hydrogen chloride, and this view was confirmed by the subsequent study in this paper.
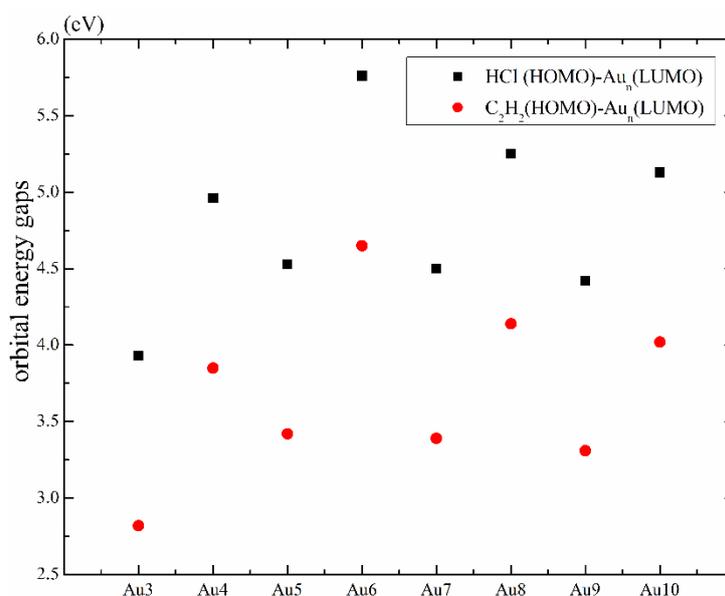

Fig. S3.The orbital energy gaps between HOMO of C_2H_2, HCl and LUMO of Au_n cluster. (energies in eV, isovalue = 0.02)

2 Adsorption and activation of C_2H_2 and HCl on Au_n (n=3–10) clusters.

By predicting the active sites on the Au_n clusters in Fig. S2, we built all possible adsorption configurations for HCl and C_2H_2 and noted the stable adsorption complexes. All complexes with no imaginary frequencies and their corresponding adsorption energies are listed in Fig. S4. The Au_3, Au_4, and Au_6 clusters have only one adsorption site, whereas the other clusters have more. The planes between HCl or C_2H_2 and $Au_{3–5}$ clusters are coplanar, whereas the planes of HCl or C_2H_2 are vertical with the $Au_{6–10}$ clusters. In Au_5 complexes, C_2H_2 is very easily adsorbed to the bridge

4

site between the Au (2) and Au (4) atoms (the code numbers of Au clusters are shown in Fig. S1), and the adsorption energy reached –22.4 kcal·mol^{-1}. However, C_2H_2 fully occupies the active site; thus, the effective adsorption of HCl in the Au$_5$ cluster is difficult. This orientation is not conducive for the reaction of both compounds. Therefore, the best adsorption configuration involves HCl and C_2H_2 sharing the
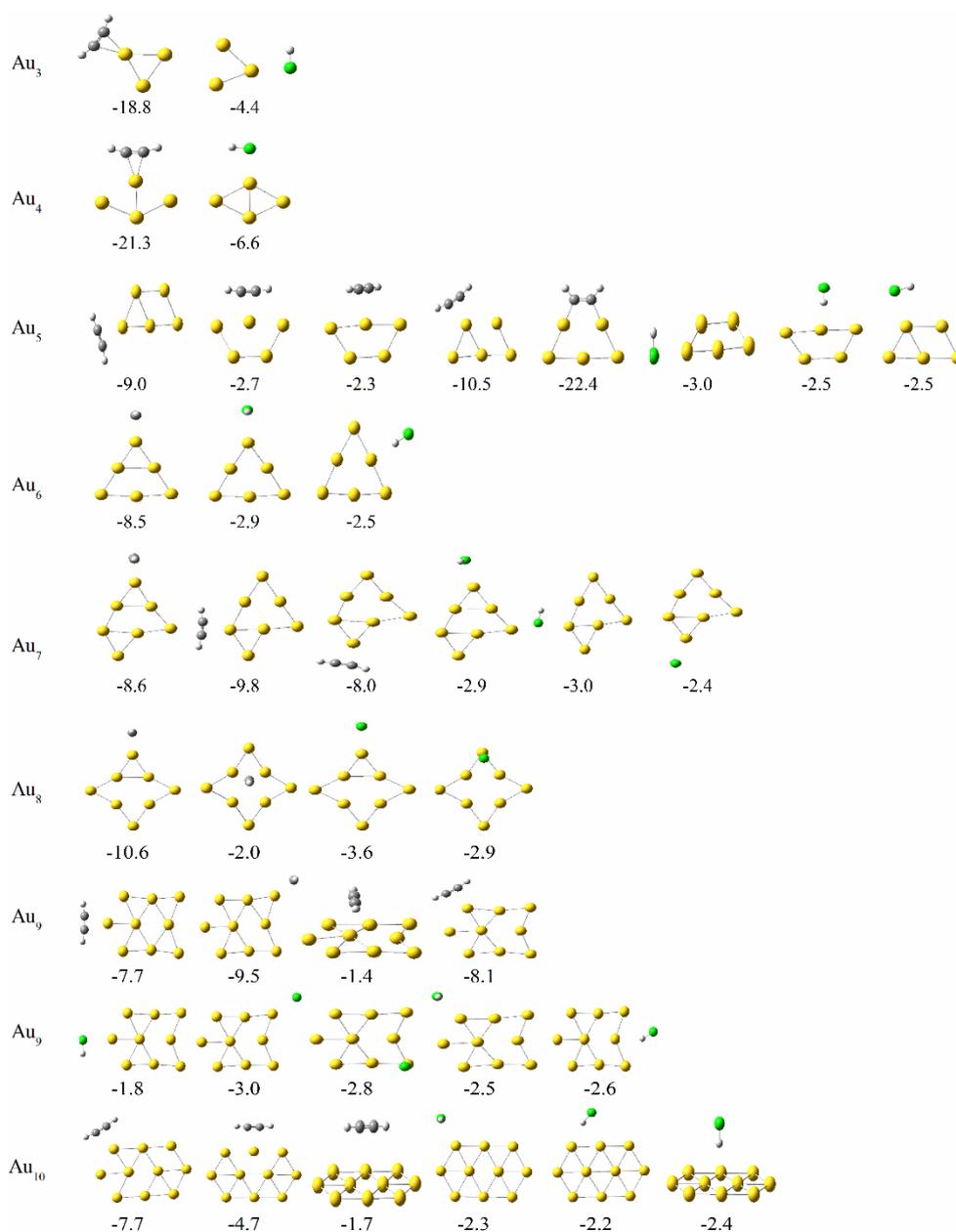

Fig. S4. The adsorption configurations and energies of C_2H_2 and HCl on different sites of Au$_n$ cluster. (energies in kcal·mol^{-1})

bridge site together, with C_2H_2 occupying the Au (2) atom and HCl occupying the Au (4) atom. C_2H_2 is conventionally much easier to adsorb on the Au_n clusters than HCl, which verifies the previous prediction. In Table S2, we show the optimal adsorption energies of C_2H_2 and HCl on the Au_n clusters, and the chart is shown in Fig. S5. The Au_n clusters would preferentially adsorb C_2H_2 to form Au_n-C_2H_2 complexes and the complexes adsorb HCl because of the considerable difference in the adsorption energies of C_2H_2 and HCl. Moreover, the adsorption energies of C_2H_2 and HCl tend to

Table S2. The optimal adsorption energies of C_2H_2, HCl on Au_{3-10} cluster. (energies in kcal·mol^{-1})

	Au_3	Au_4	Au_5	Au_6	Au_7	Au_8	Au_9	Au_{10}
C_2H_2	-18.8	-21.3	-10.5	-8.5	-9.8	-10.6	-7.7	-7.7
HCl	-4.4	-6.6	-3.0	-2.9	-3.0	-3.6	-3.0	-2.4
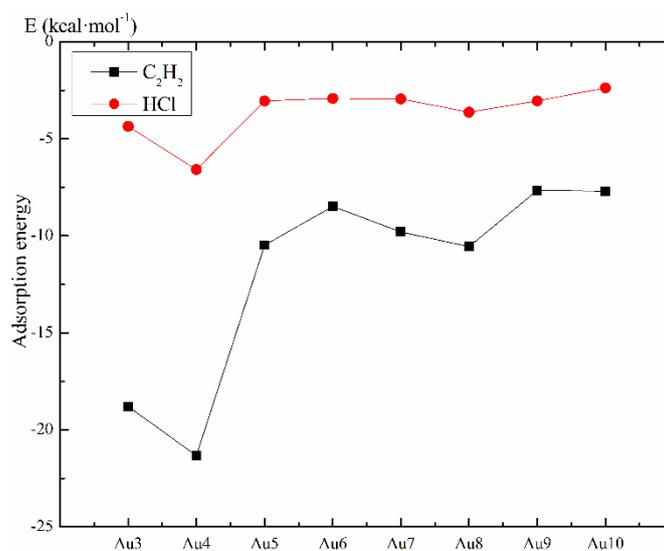
Fig. S5. The adsorption energies of C_2H_2 and HCl on Au_{3-10} cluster (energies in kcal·mol^{-1}).

remain constant. Among the Au_n (n=3-10) clusters, the Au_4 cluster shows the highest ability of adsorbing C_2H_2 and HCl. In order to better elucidate the direction of electron transfer between gold clusters and C_2H_2 / HCl in the process of adsorption, we listed the mulliken partial charges (au) of Au cluster, C_2H_2 and HCl in different adsorbed complexes. In Table S4, the Au cluster is always electron acceptor during adsorbing C_2H_2 and HCl. Both in the Au_n-C_2H_2 and Au_n-HCl adsorbed complexes, the Au clusters gathered many negative charges. That indicates the electron transfers from the HOMO of C_2H_2 and HCl to the LUMO of Au_n clusters, and this is consistent with the results of FMO analysis. Besides, Au clusters of Au_n-C_2H_2 adsorbed complexes have more negative charges and that of Au_n-HCl complexes. Now through the FMO analysis, energy gaps, adsorption energies and charge analysis, we drew a deep conclusion that C_2H_2 is a preferential adsorption on Au clusters.

3 Transition states in Au_3 cluster catalyzed reaction pathway.

The acetylene hydrochlorination catalyzed by Au_3 cluster can be achieved through two transition states, and we showed the geometries of transition states (Ts) In Fig. S6. The bond length of transition states involved in the Au_3 cluster catalysis pathways are shown in Table S5. In Ts1, the HCl is cracked by both C_2H_2 and Au_3 cluster. Therefore, the C_2H_2 and HCl are activated simultaneously, and thus this step shows synergistic effect. This activation is significantly strong because the length of H 4–Cl 5 in Ts1 is 1.493 Å (the normal bond length of HCl is just 1.286 Å). In Ts2, the H 4 atom and the chloroethenyl are both adsorbed at the Au 1 site, thereby allowing easy transfer of the H 4 atom from Au 1 to C 8 atom of C_2H_2; this can be

7

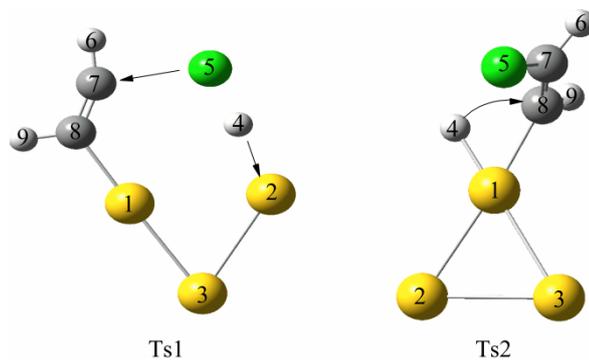inferred from the tiny energy barrier between Im1 and Ts2 (Fig. 7).

Fig. S6. The geometries of transition states (Ts) in the Au_3 cluster catalyzed reaction pathway. Au, Cl, C and H atoms are depicted in yellow, green, gray and white respectively.

Table S4. The mulliken partial charges (au) of Au cluster, C_2H_2 and HCl in different adsorbed complexes.

Components	Au_n-C_2H_2 (au)								Au_n-HCl (au)							
	Au_3	Au_4	Au_5	Au_6	Au_7	Au_8	Au_9	Au_{10}	Au_3	Au_4	Au_5	Au_6	Au_7	Au_8	Au_9	Au_{10}
Au cluster	-0.446	-0.466	-0.492	-0.431	-0.481	-0.453	-0.466	-0.495	-0.313	-0.362	-0.241	-0.219	-0.248	-0.248	-0.245	-0.213
C_2H_2	0.446	0.466	0.492	0.431	0.481	0.453	0.466	0.495	—	—	—	—	—	—	—	—
HCl	—	—	—	—	—	—	—	—	0.313	0.362	0.241	0.219	0.248	0.248	0.245	0.213

Table S5. The bond length (Å) of transition states (Ts) involved in the Au_3 cluster catalyzed reaction pathway.

Atom-Bond	1-8	4-5	7-8	5-7	4-8
Ts1	2.070	1.493	1.272	2.364	3.331
Ts2	2.067	3.240	1.334	1.741	1.805

References and Notes

1 H. Hakkinen and U. Landman, *Phys. Rev. B*, 2000, **62**, 2287-2290.

2 V. Bonacic-Koutecky, J. Burda, R. Mitric, M. Ge, G. Zampella and P. Fantucci, *J. Chem. Phys.*, 2002, **117**, 3120-3131.

3 J. Wang, G. Wang and J. Zhao, *Phys. Rev. B*, 2002, **66**, 035418-035424.

4 L. Xiao and L. Wang, *Chem. Phys. Lett.*, 2004, **392**, 452–455.

5 F. Furche, R. Ahlrichs, P. Weis, C. Jacob, S. Gilb, T. Bierweiler and M. M. Kappes, *J. Chem. Phys.*, 2002, **117**, 6982-6990.

6 X. Chen, S. Sun, F. Li , X. Wang and D. Xia, *Molecules*, 2013, **18**, 3279-3291.